Electronic Supplementary Material (ESI) for RSC Advances.

Supplementary information for "Quantitative Structure-Property Relationship Study of Reorganization Energy for p-Type Organic Semiconductors"

Sule Atahan-Evrenk*

TOBB University of Economics and Technology, Faculty of Medicine

43 Sogutozu Cad. Sogutozu Ankara TURKEY

E-mail: satahanevrenk@etu.edu.tr

September 19, 2018

1 Molecular library

Table 1: The compound set and electronic data.

	Compound	Reorganization Energy (meV)	Previous Work	ϵ_n^{homo} (eV)	ϵ_c^{homo} (eV)	IP_{adia} (eV)	IP_{vert} (eV)	References
1	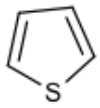	403	408[1]	−6.35	−5.98	8.51	8.71	
2	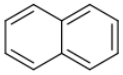	185	178[2] 182[3] 186[4] 189[5]	−5.80	−5.62	7.61	7.70	[6]
3	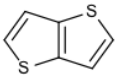	409	410[7]	−5.86	−5.47	7.66	7.87	[8]
4	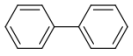	358		−6.06	−5.71	7.61	7.80	
5	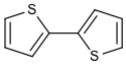	420	365[9] 424[1]	−5.54	−5.13	7.12	7.35	[9]
6	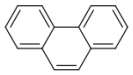	218	212[2]	−5.74	−5.53	7.32	7.43	[2]
7	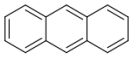	138	134[2] 138[4] 141[5]	−5.24	−5.10	6.82	6.89	[10]
8	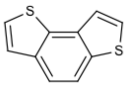	230		−5.78	−5.55	7.40	7.51	[11]
9	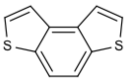	288		−5.67	−5.39	7.27	7.41	[11]
10	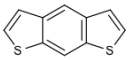	108	106[4]	−5.50	−5.39	7.15	7.20	[12]
11	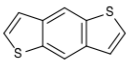	165	166[4]	−5.48	−5.31	7.11	7.19	[13]

Continued on the next page

	Compound	Reorganization Energy (meV)	Previous Work	ϵ_n^{homo} (eV)	ϵ_c^{homo} (eV)	IP_{adia} (eV)	IP_{vert} (eV)	References
12	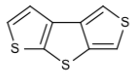	193		−5.51	−5.32	7.17	7.26	[14]
13	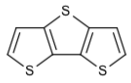	352	350[7] 350[4]	−5.61	−5.27	7.20	7.38	[15]
14	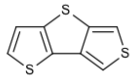	209		−5.53	−5.33	7.19	7.29	[16]
15	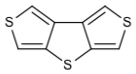	187		−5.66	−5.48	7.36	7.45	[14]
16	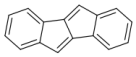	279		−5.42	−5.14	6.87	7.01	[17]
17	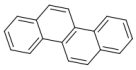	165	161[2]	−5.53	−5.36	6.95	7.04	[18]
18	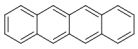	111	109[2] 114[4] 115[5]	−4.87	−4.76	6.28	6.34	[19]
19	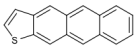	110		−4.99	−4.88	6.42	6.48	[20]
20	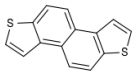	243		−5.56	−5.32	6.99	7.11	[11]
21	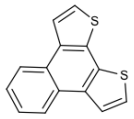	238		−5.51	−5.28	6.96	7.08	[8]
22	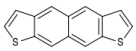	100	100[4]	−5.10	−5.01	6.57	6.62	[11]
23	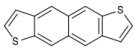	105	106[4]	−5.10	−5.00	6.56	6.61	[11]
24	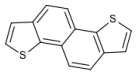	280		−5.67	−5.41	7.10	7.24	[21]
25	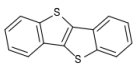	225		−5.59	−5.37	7.04	7.15	[22]

Continued on the next page

	Compound	Reorganization Energy (meV)	Previous Work	ϵ_n^{homo} (eV)	ϵ_c^{homo} (eV)	IP_{adia} (eV)	IP_{vert} (eV)	References
26	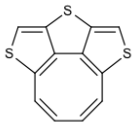	378		−5.02	−4.66	6.44	6.63	[8]
27	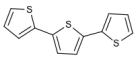	373	321[9] 373[1]	−5.20	−4.84	6.50	6.70	[9]
28	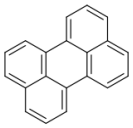	145	142[2]	−4.96	−4.83	6.36	6.43	[23]
29	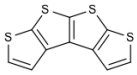	301		−5.72	−5.42	7.19	7.34	[8]
30	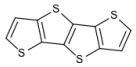	326	326[4] 330[7]	−5.43	−5.11	6.85	7.02	[15]
31	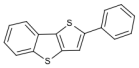	299		−5.49	−5.21	6.79	6.95	[8]
32	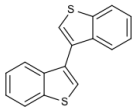	302		−5.59	−5.27	6.92	7.08	[8]
33	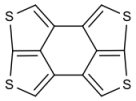	183		−5.44	−5.25	6.89	6.98	[8]
34	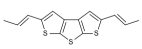	215		−5.37	−5.20	6.71	6.82	[8]
35	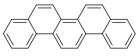	185	180[2] 180[24] 182[25]	−5.50	−5.32	6.81	6.90	[26]
36	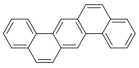	168	168[25]	−5.39	−5.23	6.70	6.78	[25]
37	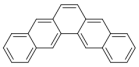	178	178[12] 177[25]	−5.33	−5.16	6.61	6.70	[12]

Continued on the next page

	Compound	Reorganization Energy (meV)	Previous Work	ϵ_n^{homo} (eV)	ϵ_c^{homo} (eV)	IP_{adia} (eV)	IP_{vert} (eV)	References
38	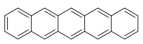	93	92[2] 95[5] 98[4] 91[24] 92[25] 91[27]	−4.61	−4.52	5.90	5.95	[28]
39	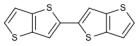	365		−5.29	−4.94	6.56	6.76	[8]
40	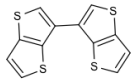	256		−5.61	−5.36	7.02	7.14	[8]
41	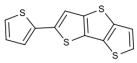	359		−5.27	−4.92	6.55	6.75	[8]
42	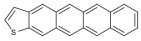	96	92.9[27]	−4.71	−4.61	6.01	6.06	[20]
43	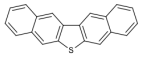	118	116[25] 119[12] 115[27]	−5.42	−5.31	6.77	6.83	[12]
44	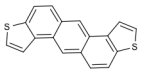	155		−5.23	−5.08	6.56	6.63	[11]
45	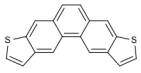	200	204[12]	−5.35	−5.16	6.65	6.75	[12]
46	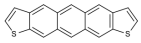	94	94[4] 90[27]	−4.81	−4.72	6.13	6.18	[29]
47	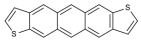	95	94[25] 96[4] 96[22] 91[27]	−4.81	−4.71	6.13	6.18	[30]
48	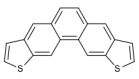	182	181[12]	−5.43	−5.25	6.76	6.84	[12]
49	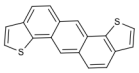	134		−5.27	−5.14	6.62	6.68	[11]
50	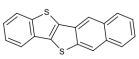	153	148[27]	−5.32	−5.17	6.66	6.73	[31]
51	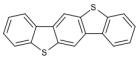	117	114[27]	−5.58	−5.46	6.97	7.02	[32]
52	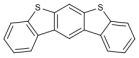	87	82.5[27]	−5.63	−5.55	7.01	7.05	[27]

Continued on the next page

	Compound	Reorganization Energy (meV)	Previous Work	ϵ_n^{homo} (eV)	ϵ_c^{homo} (eV)	IP_{adia} (eV)	IP_{vert} (eV)	References
53	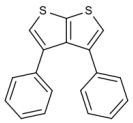	266		−5.75	−5.52	7.12	7.26	[8]
54	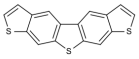	149	148[4]	−5.46	−5.32	6.82	6.89	[33]
			142[27]					
55	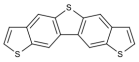	118	118[4]	−5.53	−5.41	6.92	6.98	[33]
			119[25]					
			112[27]					
56	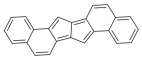	208		−4.99	−4.78	6.21	6.31	[17]
57	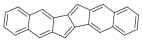	115		−5.24	−5.13	6.46	6.52	[17]
58	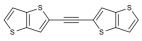	293		−5.24	−4.96	6.46	6.61	[8]
59	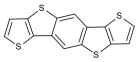	231	231[25]	−5.42	−5.19	6.75	6.86	[22]
			221[27]					
60	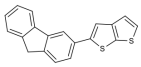	320		−5.52	−5.19	6.74	6.91	[8]
61	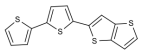	362		−5.15	−4.80	6.33	6.53	[8]
62	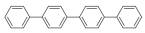	309		−5.62	−5.32	6.74	6.90	[34]
63	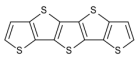	307	306[22]	−5.30	−5.00	6.61	6.76	[15]
			307[25]					
			308[4]					
			310[7]					
			314[5]					
			299[27]					
64	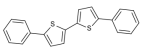	318		−5.12	−4.83	6.28	6.45	[35]
65	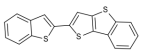	266		−5.39	−5.13	6.58	6.72	[8]
66	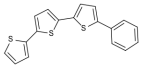	339		−5.07	−4.75	6.21	6.39	[36]

Continued on the next page

	Compound	Reorganization Energy (meV)	Previous Work	ϵ_n^{homo} (eV)	ϵ_c^{homo} (eV)	IP_{adia} (eV)	IP_{vert} (eV)	References
67	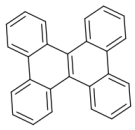	193		−5.31	−5.12	6.54	6.63	[37]
68	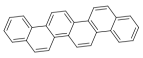	148	144[2]	−5.43	−5.28	6.64	6.72	[2]
69	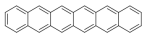	79	79[2]	−4.42	−4.34	5.61	5.65	[38]
70	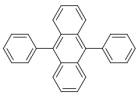	255		−5.10	−4.88	6.37	6.51	[39]
71	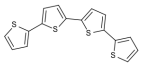	348	293[9] 345[1] 379[5]	−5.02	−4.69	6.14	6.34	[1]
72	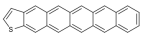	85		−4.50	−4.42	5.71	5.75	[40]
73	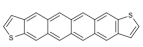	87		−4.59	−4.50	5.80	5.85	[22]
74	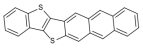	114		−5.02	−4.91	6.27	6.32	[31]
75	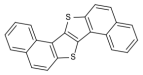	196		−5.33	−5.14	6.56	6.65	[41]
76	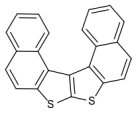	187		−5.34	−5.15	6.60	6.69	[8]
77	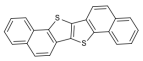	189		−5.47	−5.29	6.68	6.77	[41]
78	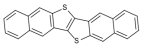	130	130[22] 134[5]	−5.19	−5.06	6.42	6.48	[42]
79	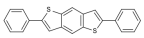	267		−5.27	−5.03	6.45	6.58	[43]
80	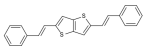	252		−4.97	−4.74	6.06	6.18	[8]
81	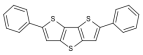	312		−5.19	−4.91	6.34	6.50	
82	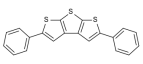	225		−5.55	−5.34	6.76	6.88	[44]
83	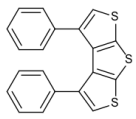	212		−5.57	−5.36	6.85	6.96	[8]

Continued on the next page

	Compound	Reorganization Energy (meV)	Previous Work	ϵ_n^{homo} (eV)	ϵ_c^{homo} (eV)	IP_{adia} (eV)	IP_{vert} (eV)	References
84	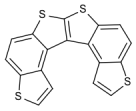	211		−5.39	−5.18	6.66	6.76	[8]
85	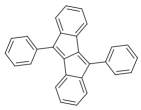	320		−5.31	−5.00	6.52	6.67	[17]
86	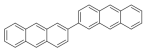	103		−5.11	−5.00	6.23	6.28	[45]
87	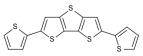	328		−5.07	−4.76	6.19	6.37	[46]
88	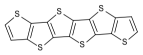	291	290[7]	−5.21	−4.93	6.42	6.56	[47]
89	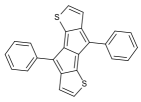	414		−4.76	−4.36	5.93	6.13	[48]
90	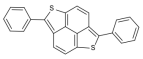	160		−4.72	−4.58	5.92	6.00	[49]
91	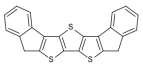	237	245[5]	−5.19	−4.95	6.38	6.50	[50]
92	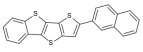	262		−5.30	−5.05	6.42	6.55	[8]
93	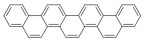	152	148[2]	−5.41	−5.26	6.55	6.63	[2]
94	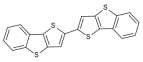	281		−5.29	−5.01	6.39	6.55	[8]
95	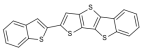	264		−5.30	−5.04	6.41	6.55	[51]
96	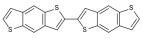	230		−5.31	−5.08	6.42	6.53	[52]
97	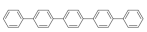	288		−5.54	−5.25	6.54	6.69	[34]
98	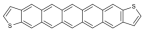	79		−4.42	−4.34	5.55	5.59	[22]
99	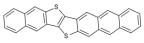	103		−4.98	−4.88	6.14	6.19	[31]
100	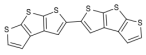	372		−5.39	−5.01	6.50	6.71	[53]
101	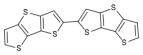	337		−5.14	−4.81	6.22	6.41	[54]
102	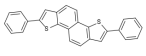	253		−5.32	−5.09	6.41	6.53	[55]
103	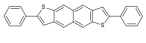	155		−5.00	−4.87	6.18	6.25	[55]
104	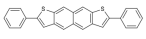	116		−5.02	−4.92	6.23	6.28	[55]

Continued on the next page

	Compound	Reorganization Energy (meV)	Previous Work	ϵ_n^{homo} (eV)	ϵ_c^{homo} (eV)	IP_{adia} (eV)	IP_{vert} (eV)	References
105	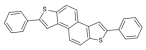	232		−5.30	−5.09	6.42	6.53	[55]
106	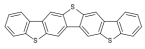	106		−5.50	−5.39	6.71	6.76	[56]
107	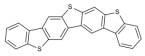	110		−5.55	−5.43	6.75	6.81	[56]
108	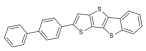	292		−5.29	−5.02	6.37	6.52	[8]
109	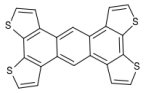	132		−5.21	−5.08	6.40	6.47	[39]
110	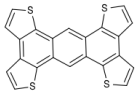	124		−5.30	−5.18	6.51	6.57	[32]
111	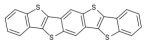	179		−5.34	−5.16	6.50	6.58	[57]
112	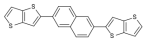	305		−5.26	−4.96	6.27	6.43	[58]
113	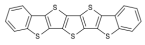	241		−5.31	−5.07	6.43	6.56	[59]
114	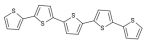	309	272[9] 314[1]	−4.90	−4.61	5.91	6.07	[60]
115	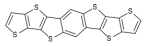	236		−5.26	−5.03	6.39	6.51	[57]
116	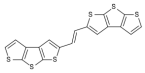	308		−5.14	−4.83	6.24	6.39	[53]
117	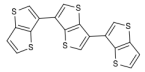	160		−5.58	−5.42	6.79	6.87	[8]
118	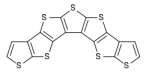	207		−5.55	−5.35	6.77	6.87	[8]
119	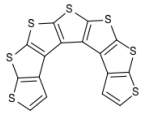	210		−5.62	−5.42	6.86	6.98	[8]
120	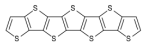	280	280[4]	−5.14	−4.87	6.27	6.41	[15]
121	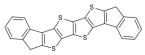	134		−4.98	−4.86	6.05	6.12	[8]
122	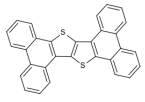	186		−5.32	−5.14	6.42	6.51	[61]
123	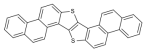	181		−5.33	−5.15	6.42	6.51	[61]

Continued on the next page

	Compound	Reorganization Energy (meV)	Previous Work	ϵ_n^{homo} (eV)	ϵ_c^{homo} (eV)	IP_{adia} (eV)	IP_{vert} (eV)	References
124	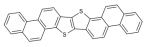	181		−5.45	−5.27	6.53	6.62	[61]
125	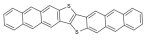	85		−4.89	−4.81	5.96	6.00	[61]
126		311		−5.19	−4.90	6.18	6.34	[8]
127	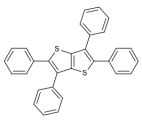	290		−5.25	−4.97	6.32	6.47	[8]
128	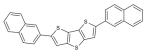	261		−5.11	−4.87	6.13	6.26	
129	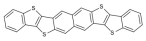	124		−5.12	−5.00	6.24	6.30	[31]
130	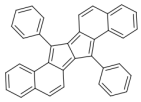	242		−4.89	−4.66	5.97	6.09	[17]
131	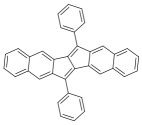	141		−5.06	−4.93	6.13	6.20	[17]
132	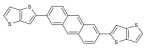	240		−5.10	−4.87	6.09	6.22	[58]
133	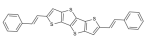	232		−4.91	−4.70	5.89	6.00	[8]
134	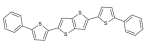	301		−4.95	−4.67	5.91	6.08	[8]
135	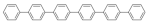	254		−5.49	−5.23	6.41	6.53	[34]
136	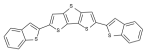	257		−5.15	−4.90	6.15	6.28	[8]
137	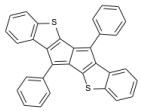	348		−4.71	−4.37	5.73	5.90	[48]
138	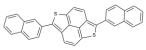	165		−4.70	−4.55	5.76	5.84	[49]
139	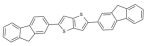	300		−5.05	−4.76	6.00	6.15	[8]
140	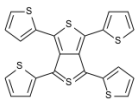	182		−4.51	−4.35	5.62	5.72	[8]
141	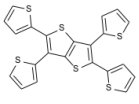	452		−5.22	−4.75	6.18	6.43	[8]
142	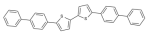	309		−5.06	−4.78	6.02	6.19	[62]

Continued on the next page

	Compound	Reorganization Energy (meV)	Previous Work	ϵ_n^{homo} (eV)	ϵ_c^{homo} (eV)	IP_{adia} (eV)	IP_{vert} (eV)	References
143	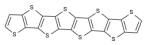	268		−5.09	−4.83	6.15	6.28	[8]
144	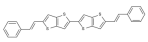	232		−4.85	−4.64	5.78	5.89	[8]
145	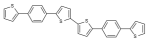	323		−5.01	−4.71	5.92	6.09	[63]
146	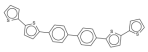	287		−5.12	−4.84	5.99	6.15	[64]
147	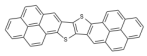	76		−5.21	−5.14	6.27	6.31	[61]
148	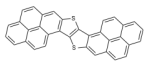	140		−4.92	−4.79	5.95	6.02	[61]
149	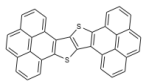	123		−5.17	−5.05	6.24	6.30	[61]
150	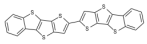	270		−5.15	−4.89	6.14	6.28	[51]
151	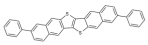	145		−5.14	−5.01	6.19	6.26	[65]
152	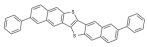	108		−5.19	−5.08	6.29	6.35	[65]
153	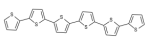	258	253[9] 301[1]	−4.81	−4.56	5.74	5.87	[66]
154	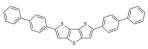	293		−5.11	−4.85	6.07	6.23	[46]
155	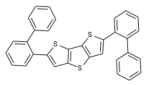	305		−5.12	−4.84	6.17	6.33	[8]
156	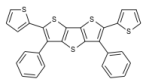	481		−5.11	−4.63	6.02	6.28	[8]
157	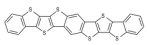	205		−5.29	−5.09	6.30	6.40	[8]
158	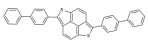	181		−4.69	−4.54	5.73	5.82	[49]
159	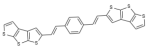	257		−5.02	−4.76	5.96	6.08	[8]
160	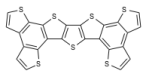	199		−5.22	−5.02	6.27	6.37	[67]
161	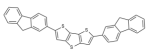	275		−4.99	−4.73	5.92	6.06	[8]
162	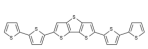	290		−4.88	−4.61	5.77	5.94	[8]
163	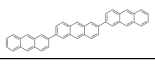	83		−5.04	−4.95	5.95	5.99	[45]

Continued on the next page

	Compound	Reorganization Energy (meV)	Previous Work	ϵ_n^{homo} (eV)	ϵ_c^{homo} (eV)	IP_{adia} (eV)	IP_{vert} (eV)	References
164	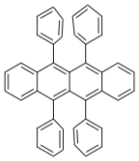	147	160[5]	−4.69	−4.56	5.80	5.87	[68]
165	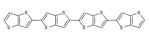	301		−4.94	−4.65	5.81	5.97	[8]
166	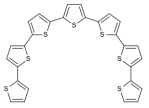	265	273[1]	−4.78	−4.54	5.63	5.76	[15]
167	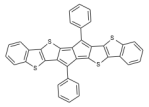	308		−4.72	−4.42	5.66	5.81	[48]
168	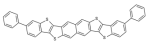	133		−5.11	−4.98	6.12	6.19	[8]
169	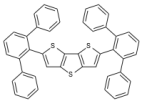	363		−5.13	−4.80	6.12	6.31	[8]
170	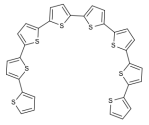	268	256[1]	−4.77	−4.52	5.54	5.68	[9]
171	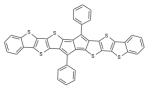	266		−4.67	−4.41	5.55	5.68	[48]

Table 2: Pairwise correlation matrix with Pearson's correlation coefficient for the RE (λ) and electronic and structural descriptors.

	λ	E_n	ϵ_n^{homo}	ϵ_c^{homo}	ϵ_n^{lumo}	ϵ_c^{lumo}	IP$_{vert}$	QPol$_{ave}$	FsdRing	RotBond	Scount	vdWsa	Rcount
λ	1.00	-0.26	-0.20	0.08	0.16	0.05	0.19	-0.05	-0.46	0.44	0.34	-0.05	-0.22
E_n	-0.26	1.00	-0.32	-0.40	0.30	0.30	0.48	-0.64	-0.24	-0.43	-0.93	-0.48	-0.60
ϵ_n^{homo}	-0.20	-0.32	1.00	0.96	-0.87	-0.86	-0.94	0.64	0.20	0.35	0.13	0.55	0.52
ϵ_c^{homo}	0.08	-0.40	0.96	1.00	-0.84	-0.86	-0.90	0.64	0.08	0.47	0.23	0.54	0.47
ϵ_n^{lumo}	0.16	0.30	-0.87	-0.84	1.00	0.99	0.85	-0.65	-0.31	-0.24	-0.10	-0.50	-0.57
ϵ_c^{lumo}	0.05	0.30	-0.86	-0.86	0.99	1.00	0.84	-0.66	-0.23	-0.32	-0.10	-0.52	-0.54
IP$_{vert}$	0.19	0.48	-0.94	-0.90	0.85	0.84	1.00	-0.82	-0.29	-0.46	-0.22	-0.75	-0.71
QPol$_{ave}$	-0.05	-0.64	0.64	0.64	-0.65	-0.66	-0.82	1.00	0.28	0.62	0.33	0.92	0.84
FsdRing	-0.46	-0.24	0.20	0.08	-0.31	-0.23	-0.29	0.28	1.00	-0.50	0.12	0.23	0.68
RotBond	0.44	-0.43	0.35	0.47	-0.24	-0.32	-0.46	0.62	-0.50	1.00	0.26	0.65	0.21
Scount	0.34	-0.93	0.13	0.23	-0.10	-0.10	-0.22	0.33	0.12	0.26	1.00	0.13	0.30
vdWsa	-0.05	-0.48	0.55	0.54	-0.50	-0.52	-0.75	0.92	0.23	0.65	0.13	1.00	0.83
Rcount	-0.22	-0.60	0.52	0.47	-0.57	-0.54	-0.71	0.84	0.68	0.21	0.30	0.83	1.00

E_n: Total electronic energy, ϵ: Molecular orbital energy, IP$_{vert}$: Vertical Ionization Potential, QPol$_{ave}$: Average polarizability, FsdRing: Fused ring count, RotBond: Rotatable bond count,Scount: Sulfur atom count, vdWsa: van der Waals surface area, Rcount: Ring count Electronic descriptors calculated at the B3LYP/6-31G(d,p) level of theory.

2 Molecular transform descriptors

Following Soltzberg and Wilkins, we limit s into the interval $[1, 31]$ divided into 100 equal pieces. However, instead of the binary representation they used in which the intervals with $I(s) = 0$ were coded as "1", and "0" otherwise, we retained the original $I(s)$ values. Figure 1 plots the comparison of $I(s)$ distributions for the pentacene with the DFT and molecular mechanics (MM) geometries.

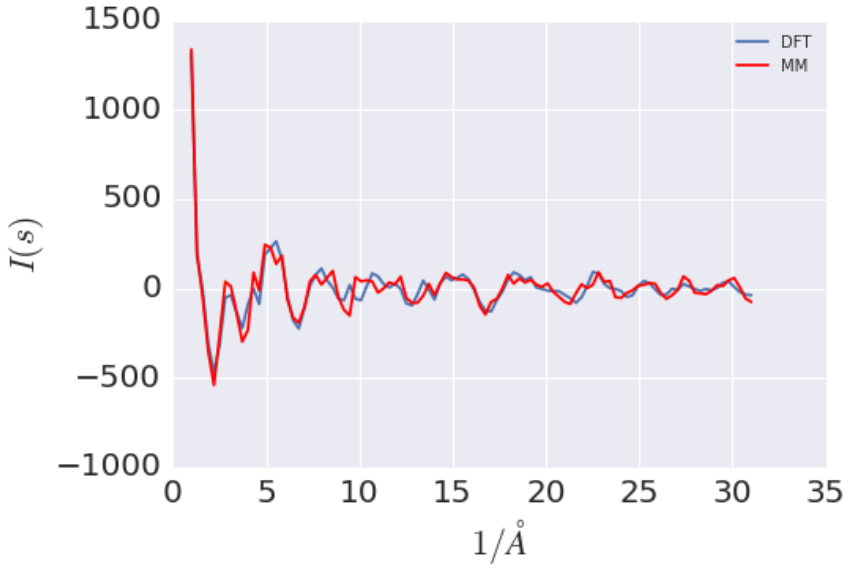

Figure 1: $3D$ structural descriptor based on the molecular transforms for pentacene with the DFT and MM geometries.

3 Principle Components

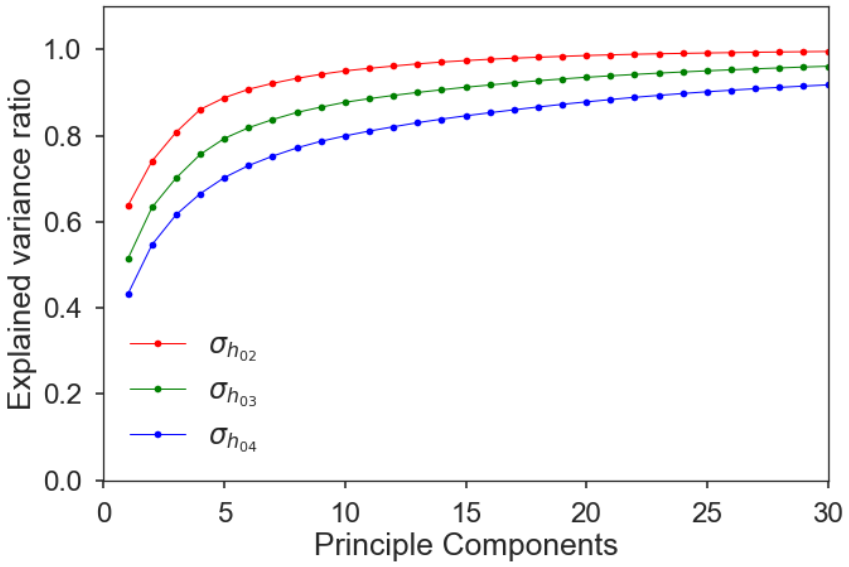

Figure 2: Explained variance ratio by the principle components in the signature (*left*) descriptor spaces

References

(1) da Silva Filho, D. A.; Coropceanu, V.; Fichou, D.; Gruhn, N. E.; Bill, T. G.; Gierschner, J.; Cornil, J.; Brédas, J.-L. Hole-vibronic coupling in oligothiophenes: impact of backbone torsional flexibility on relaxation energies. *Philos. Trans. R. Soc., A* **2007**, *365*, 1435–1452.

(2) Malloci, G.; Cappellini, G.; Mulas, G.; Mattoni, A. Electronic and optical properties of families of polycyclic aromatic hydrocarbons: A systematic (time-dependent) density functional theory study. *Chem. Phys.* **2011**, *384*, 19 – 27.

(3) Malloci, G.; Mulas, G.; Cappellini, G.; Joblin, C. Time-dependent density functional study of the electronic spectra of oligoacenes in the charge states $1, 0, +1$, and $+2$. *Chem. Phys.* **2007**, *340*, 43 – 58.

(4) Coropceanu, V.; Cornil, J.; Filho, D. S.; A, D.; Olivier, Y.; Silbey, R.; Brédas, J.-L. Charge transport in organic semiconductors. *Chem. Rev* **2007**, *107*, 926–952.

(5) Yavuz, I.; Martin, B. N.; Park, J.; Houk, K. N. Theoretical Study of the Molecular Ordering, Paracrystallinity, And Charge Mobilities of Oligomers in Different Crystalline Phases. *J. Am. Chem. Soc.* **2015**, *137*, 2856–2866.

(6) Karl, N. Charge carrier transport in organic semiconductors. *Synthetic Metals* **2003**, *133*, 649 – 657, Proceedings of the Yamada Conference LVI. The Fourth International Symposium on Crystalline Organic Metals, Superconductors and Ferromagnets (ISCOM 2001).

(7) Zhang, Y.; Cai, X.; Bian, Y.; Li, X.; Jiang, J. Heteroatom Substitution of Oligothienoacenes: From Good p-Type Semiconductors to Good Ambipolar Semiconductors for Organic Field-Effect Transistors. *J. Phys. Chem. C* **2008**, *112*, 5148–5159.

(8) Cinar, M. E.; Ozturk, T. Thienothiophenes, Dithienothiophenes, and Thienoacenes: Syntheses, Oligomers, Polymers, and Properties. *Chem. Rev.* **2015**, *115*, 3036–3140.

(9) Hutchison, G. R.; Ratner, M. A.; Marks, T. J. Hopping Transport in Conductive Heterocyclic Oligomers: Reorganization Energies and Substituent Effects. *J. Am. Chem. Soc.* **2005**, *127*, 2339–2350.

(10) Aleshin, A. N.; Lee, J. Y.; Chu, S. W.; Kim, J. S.; Park, Y. W. Mobility studies of field-effect transistor structures basedon anthracene single crystals. *Appl. Phys. Lett.* **2004**, *84*, 5383–5385.

(11) Osaka, I.; Shinamura, S.; Abe, T.; Takimiya, K. Naphthodithiophenes as building units for small molecules to polymers; a case study for in-depth understanding of structure-property relationships in organic semiconductors. *J. Mater. Chem. C* **2013**, *1*, 1297–1304.

(12) Coropceanu, V.; Kwon, O.; Wex, B.; Kaafarani, B. R.; Gruhn, N. E.; Durivage, J. C.; Neckers, D. C.; Brédas, J.-L. Vibronic Coupling in Organic Semiconductors: The Case of Fused Polycyclic Benzene-Thiophene Structures. *Chem. Eur. J.* **2006**, *12*, 2073–2080.

(13) Tomoya, K.; Eigo, M.; Kazuo, T. 2,6-Dialkylbenzo[1,2-b:4,5-b']dithiophenes (Cn-BDTs) as Soluble Organic Semiconductors for Solution-processed Organic Field-effect Transistors. *Chem. Lett.* **2008**, *37*, 284–285.

(14) Janssen, M. J.; De Jong, F. Synthesis, oxidation, and electronic spectra of four dithienothiophenes. *J. Org. Chem.* **1971**, *36*, 1645–1648.

(15) Zhang, X.; Cote, A. P.; Matzger, A. J. Synthesis and Structure of Fused alpha-Oligothiophenes with up to Seven Rings. *J. Am. Chem. Soc.* **2005**, *127*, 10502–10503.

(16) De Jong, F.; Janssen, M. J. Synthesis of dithienothiophenes. *J. Org. Chem.* **1971**, *36*, 1998–2000.

(17) Kawase, T.; Fujiwara, T.; Kitamura, C.; Konishi, A.; Hirao, Y.; Matsumoto, K.; Kurata, H.; Kubo, T.; Shinamura, S.; Mori, H.; Miyazaki, E.; Takimiya, K. Dinaphthopentalenes: Pentalene Derivatives for Organic Thin-Film Transistors. *Angew. Chem. Int. Ed.* **2010**, *49*, 7728–7732.

(18) Kunugi, Y.; Ikari, M.; Okamoto, K. Chrysene Derivatives as New Organic Semiconductors for Organic Field-effect Transistors. *ECS Trans.* **2010**, *25*, 11–17.

(19) Goldmann, C.; Haas, S.; Krellner, C.; Pernstich, K. P.; Gundlach, D. J.; Batlogg, B. Hole

mobility in organic single crystals measured by a flip-crystal field-effect technique. *J. Appl. Phys.* **2004**, *96*, 2080–2086.

(20) Tang, M. L.; Okamoto, T.; Bao, Z. High-Performance Organic Semiconductors:âĂĽ Asymmetric Linear Acenes Containing Sulphur. *J. Am. Chem. Soc.* **2006**, *128*, 16002–16003.

(21) Shinamura, S.; Miyazaki, E.; Takimiya, K. Synthesis, Properties, Crystal Structures, and Semiconductor Characteristics of Naphtho[1,2-b:5,6-b']dithiophene and -diselenophene Derivatives. *J. Org. Chem.* **2010**, *75*, 1228–1234.

(22) Takimiya, K.; Shinamura, S.; Osaka, I.; Miyazaki, E. Thienoacene-Based Organic Semiconductors. *Adv. Mater.* **2011**, *23*, 4347–4370.

(23) Kim, S. H.; Yang, Y. S.; Lee, J. H.; Lee, J.-I.; Chu, H. Y.; Lee, H.; Oh, J.; Do, L.-M.; Zyung, T. Organic field-effect transistors using perylene. *Opt. Mater.* **2003**, *21*, 439 – 443.

(24) Nguyen, T. P.; Shim, J. H.; Lee, J. Y. Density Functional Theory Studies of Hole Mobility in Picene and Pentacene Crystals. *J. Phys. Chem. C* **2015**, *119*, 11301–11310.

(25) Mamada, M.; Yamashita, Y. *Polycyclic Arenes and Heteroarenes*; Wiley-VCH Verlag GmbH & Co. KGaA, 2015; pp 277–308.

(26) Okamoto, H.; Kawasaki, N.; Kaji, Y.; Kubozono, Y.; Fujiwara, A.; Yamaji, M. Air-assisted High-performance Field-effect Transistor with Thin Films of Picene. *J. Am. Chem. Soc.* **2008**, *130*, 10470–10471.

(27) Zhu, R.; Duan, Y.-A.; Geng, Y.; Wei, C.-Y.; Chen, X.-Y.; Liao, Y. Theoretical evaluation on the reorganization energy of five-ring-fused benzothiophene derivatives. *Comp. Theor. Chem.* **2016**, *1078*, 16–22.

(28) Knipp, D.; Street, R. A.; Völkel, A.; Ho, J. Pentacene thin film transistors on inorganic dielectrics: Morphology, structural properties, and electronic transport. *J. Appl. Phys.* **2003**, *93*, 347–355.

(29) Lehnherr, D.; Waterloo, A. R.; Goetz, K. P.; Payne, M. M.; Hampel, F.; Anthony, J. E.; Jurchescu, O. D.; Tykwinski, R. R. Isomerically Pure syn-Anthradithiophenes: Synthesis, Properties, and FET Performance. *Org. Lett.* **2012**, *14*, 3660–3663.

(30) Laquindanum, J. G.; Katz, H. E.; Lovinger, A. J. Synthesis, Morphology, and Field-Effect Mobility of Anthradithiophenes. *J. Am. Chem. Soc.* **1998**, *120*, 664–672.

(31) Mori, T.; Nishimura, T.; Yamamoto, T.; Doi, I.; Miyazaki, E.; Osaka, I.; Takimiya, K. Consecutive Thiophene-Annulation Approach to π-Extended Thienoacene-Based Organic Semiconductors with [1]Benzothieno[3,2-b][1]benzothiophene (BTBT) Substructure. *J. Am. Chem. Soc.* **2013**, *135*, 13900–13913.

(32) Liu, W.-J.; Zhou, Y.; Ma, Y.; Cao, Y.; Wang, J.; Pei, J. Thin Film Organic Transistors from Air-Stable Heteroarenes: Anthra[1,2-b:4,3-b':5,6-b":8,7-b"']tetrathiophene Derivatives. *Org. Lett.* **2007**, *9*, 4187–4190.

(33) Wex, B.; Kaafarani, B. R.; Schroeder, R.; Majewski, L. A.; Burckel, P.; Grell, M.; Neckers, D. C. New organic semiconductors and their device performance as a function of thiophene orientation. *J. Mater. Chem.* **2006**, *16*, 1121–1124.

(34) Gundlach, D. J.; Lin, Y.-Y.; Jackson, T. N.; Schlom, D. G. Oligophenyl-based organic thin film transistors. *Appl. Phys. Lett.* **1997**, *71*, 3853–3855.

(35) Katz, H. E.; Lovinger, A. J.; Hong, X. M.; Dodabalapur, A.; Johnson, J.; Wang, B.-C.; Raghavachari, K. Design of organic transistor semiconductors for logic elements, displays, and sensors. *Proc. SPIE* **2001**, *4466*, 20–30.

(36) Funahashi, M.; Kato, T. Design of liquid crystals: from a nematogen to thiophene-based π-conjugated mesogens. *Liq. Cryst.* **2015**, *42*, 909–917.

(37) Ueda, Y.; Tsuji, H.; Tanaka, H.; Nakamura, E. Synthesis, Crystal Packing, and Ambipolar Carrier Transport Property of Twisted Dibenzo[g,p]chrysenes. *Chem. - Asian J* **2014**, *9*, 1623–1628.

(38) Watanabe, M.; Chang, Y. J.; Liu, S.-W.; Chao, T.-H.; Goto, K.; Minarul, I.; Yuan, C.-H.; Tao, Y.-T.; Shinmyozu, T.; Chow, T. J. The synthesis, crystal structure and charge-transport properties of hexacene. *Nat Chem* **2012**, *4*, 574–578.

(39) Brusso, J. L.; Hirst, O. D.; Dadvand, A.; Ganesan, S.; Cicoira, F.; Robertson, C. M.; Oakley, R. T.; Rosei, F.; Perepichka, D. F. Two-Dimensional Structural Motif in Thienoacene Semiconductors: Synthesis, Structure, and Properties of Tetrathienoanthracene Isomers. *Chem. Mater.* **2008**, *20*, 2484–2494.

(40) Tang, M. L.; Mannsfeld, S. C. B.; Sun, Y.-S.; Becerril, H. A.; Bao, Z. Pentaceno[2,3-b]thiophene, a Hexacene Analogue for Organic Thin Film Transistors. *J. Am. Chem. Soc.* **2009**, *131*, 882–883.

(41) Yamamoto, T.; Shinamura, S.; Miyazaki, E.; Takimiya, K. Three Structural Isomers of Dinaphthothieno[3,2-b]thiophenes: Elucidation of Physicochemical Properties, Crystal Structures, and Field-Effect Transistor Characteristics. *Bull. Chem. Soc. Jpn.* **2010**, *83*, 120–130.

(42) Yamamoto, T.; Takimiya, K. Facile Synthesis of Highly -Extended Heteroarenes, Dinaphtho[2,3-b:2',3'-f]chalcogenopheno[3,2-b]chalcogenophenes, and Their Application to Field-Effect Transistors. *J. Am. Chem. Soc.* **2007**, *129*, 2224.

(43) Takimiya, K.; Kunugi, Y.; Konda, Y.; Niihara, N.; Otsubo, T. 2,6-Diphenylbenzo[1,2-b:4,5-b']dichalcogenophenes: A New Class of High-Performance Semiconductors for Organic Field-Effect Transistors. *J. Am. Chem. Soc.* **2004**, *126*, 5084–5085.

(44) Shi, J.; Li, Y.; Jia, M.; Xu, L.; Wang, H. Organic semiconductors based on annelated [small beta]-oligothiophenes and its application for organic field-effect transistors. *J. Mater. Chem.* **2011**, *21*, 17612–17614.

(45) Ito, K.; Suzuki, T.; Sakamoto, Y.; Kubota, D.; Inoue, Y.; Sato, F.; Tokito, S. Oligo(2,6-anthrylene)s: Acene-Oligomer Approach for Organic Field-Effect Transistors. *Angew. Chem. Int. Ed.* **2003**, *42*, 1159–1162.

(46) Sun, Y.; Ma, Y.; Liu, Y.; Lin, Y.; Wang, Z.; Wang, Y.; Di, C.; Xiao, K.; Chen, X.; Qiu, W.; Zhang, B.; Yu, G.; Hu, W.; Zhu, D. High-Performance and Stable Organic Thin-Film Transistors Based on Fused Thiophenes. *Adv. Funct. Mater.* **2006**, *16*, 426–432.

(47) Liu, Y.; Sun, X.; Di, C.-a.; Liu, Y.; Du, C.; Lu, K.; Ye, S.; Yu, G. Hexathienoacene: Synthesis, Characterization, and Thin-Film Transistors. *Chem. - Asian J.* **2010**, *5*, 1550–1554.

(48) Dai, G.; Chang, J.; Shi, X.; Zhang, W.; Zheng, B.; Huang, K.-W.; Chi, C. Thienoacene-Fused Pentalenes: Syntheses, Structures, Physical Properties and Applications for Organic Field-Effect Transistors. *Chem. - Eur. J.* **2015**, *21*, 2019–2028.

(49) Yoshihito, K.; Kazuo, T.; Kazuo, Y.; Yoshio, A.; Tetsuo, O. Organic Field-Effect Transistors Using Di(2-thienyl)naphthodithiophenes as Active Layers. *Chem. Lett.* **2002**, *31*, 958–959.

(50) Afonina, I.; Skabara, P. J.; Vilela, F.; Kanibolotsky, A. L.; Forgie, J. C.; Bansal, A. K.; Turnbull, G. A.; Samuel, I. D. W.; Labram, J. G.; Anthopoulos, T. D.; Coles, S. J.; Hursthouse, M. B. Synthesis and characterisation of new diindenodithienothiophene (DITT) based materials. *J. Mater. Chem.* **2010**, *20*, 1112–1116.

(51) Huang, P.-Y.; Chen, L.-H.; Kim, C.; Chang, H.-C.; Liang, Y.-j.; Feng, C.-Y.; Yeh, C.-M.; Ho, J.-C.; Lee, C.-C.; Chen, M.-C. High-Performance Bottom-Contact Organic Thin-Film Transistors Based on Benzo[d,d']thieno[3,2-b;4,5-b']dithiophenes (BTDTs) Derivatives. *ACS Appl. Mater. Interfaces* **2012**, *4*, 6992–6998.

(52) Laquindanum, J. G.; Katz, H. E.; Lovinger, A. J.; Dodabalapur, A. Benzodithiophene Rings as Semiconductor Building Blocks. *Adv. Mater.* **1997**, *9*, 36–39.

(53) Tan, L.; Zhang, L.; Jiang, X.; Yang, X.; Wang, L.; Wang, Z.; Li, L.; Hu, W.; Shuai, Z.; Li, L.; Zhu, D. A Densely and Uniformly Packed Organic Semiconductor Based on Annelated beta-Trithiophenes for High-Performance Thin Film Transistors. *Adv. Funct. Mater.* **2009**, *19*, 272–276.

(54) Bao, Z.; A. Rogers, J.; E. Katz, H. Printable organic and polymeric semiconducting materials and devices. *J. Mater. Chem.* **1999**, *9*, 1895–1904.

(55) Shinamura, S.; Osaka, I.; Miyazaki, E.; Nakao, A.; Yamagishi, M.; Takeya, J.; Takimiya, K. Linear- and Angular-Shaped Naphthodithiophenes: Selective Synthesis, Properties, and Application to Organic Field-Effect Transistors. *J. Am. Chem. Soc.* **2011**, *133*, 5024–5035.

(56) Sirringhaus, H.; H. Friend, R.; Wang, C.; Leuninger, J.; Mullen, K. Dibenzothienobisbenzothiophene-a novel fused-ring oligomer with high field-effect mobility. *J. Mater. Chem.* **1999**, *9*, 2095–2101.

(57) Seok, Y. Y.; Takuma, Y.; Chihaya, A. Organic Single-Crystal Transistors Based on *pi*-Extended Heteroheptacene Microribbons. *Bull. Chem. Soc. Jpn.* **2012**, *85*, 1186–1191.

(58) Kim, H.-S.; Kim, Y.-H.; Kim, T.-H.; Noh, Y.-Y.; Pyo, S.; Yi, M. H.; Kim, D.-Y.; Kwon, S.-K. Synthesis and Studies on 2-Hexylthieno[3,2-b]thiophene End-Capped Oligomers for OTFTs. *Chem. Mater.* **2007**, *19*, 3561–3567.

(59) Okamoto, T.; Kudoh, K.; Wakamiya, A.; Yamaguchi, S. General Synthesis of Thiophene and Selenophene-Based Heteroacenes. *Org. Lett.* **2005**, *7*, 5301–5304.

(60) Tasaka, S.; Katz, H.; Hutton, R.; Orenstein, J.; Fredrickson, G.; Wang, T. Electrical conductivity of α-quinquethiophene/stearic acid Langmuir-Blodgett films doped with iodine. *Synth. Met.* **1986**, *16*, 17 – 30.

(61) Sokolov, A. N.; Atahan-Evrenk, S.; Mondal, R.; Akkerman, H. B.; Sánchez-Carrera, R. S.; Granados-Focil, S.; Schrier, J.; Mannsfeld, S. C. B.; Zoombelt, A. P.; Bao, Z.; Aspuru-Guzik, A. From computational discovery to experimental characterization of a high hole mobility organic crystal. *Nat. Commun.* **2011**, *2*, 437–8.

(62) Yanagi, H.; Araki, Y.; Ohara, T.; Hotta, S.; Ichikawa, M.; Taniguchi, Y. Comparative Carrier Transport Characteristics in Organic Field-Effect Transistors with Vapor-Deposited Thin Films and Epitaxially Grown Crystals of Biphenyl-Capped Thiophene Oligomers. *Adv. Funct. Mater.* **2003**, *13*, 767–773.

(63) Facchetti, A.; Yoon, M.-H.; Katz, H. E.; Marks, T. J. Materials for n-type organic electronics: synthesis and properties of fluoroarene-thiophene semiconductors. 2003.

(64) Yoon, M.-H.; Facchetti, A.; Stern, C. E.; Marks, T. J. Fluorocarbon-Modified Organic Semiconductors: Molecular Architecture, Electronic, and Crystal Structure Tuning of Arene- versus Fluoroarene-Thiophene Oligomer Thin-Film Properties. *J. Am. Chem. Soc.* **2006**, *128*, 5792–5801.

(65) Kang, M. J.; Miyazaki, E.; Osaka, I.; Takimiya, K.; Nakao, A. Diphenyl Derivatives of Dinaphtho[2,3-b:2',3'-f]thieno[3,2-b]thiophene: Organic Semiconductors for Thermally Stable Thin-Film Transistors. *ACS Appl. Mater. Interfaces* **2013**, *5*, 2331–2336.

(66) Peng, X.; Horowitz, G.; Fichou, D.; Garnier, F. All-organic thin-film transistors made of alpha-sexithienyl semiconducting and various polymeric insulating layers. *Appl. Phys. Lett.* **1990**, *57*, 2013.

(67) Zhang, S.; Guo, Y.; Zhang, Y.; Liu, R.; Li, Q.; Zhan, X.; Liu, Y.; Hu, W. Synthesis, self-assembly, and solution-processed nanoribbon field-effect transistor of a fused-nine-ring thienoacene. *Chem. Commun.* **2010**, *46*, 2841–2843.

(68) Podzorov, V.; Sysoev, S.; Loginova, E.; Pudalov, V.; Gershenson, M. Single-crystal organic field effect transistors with the hole mobility ≈ 8 cm^2/Vs. *Appl. Phys. Lett.* **2003**, *83*, 3504.